Implementation of skeletal muscle model with advanced activation control

H. Kocková[a,*], R. Cimrman[b]

[a]*New Technologies – Research Centre in the Westbohemian Region, University of West Bohemia, Univerzitní 22, 306 14 Plzeň, Czech Republic*

[b]*Department of Mechanics, Faculty of Applied Sciences, University of West Bohemia, Univerzitní 22, 306 14 Plzeň, Czech Republic*

Abstract

The paper summarizes main principles of an advanced skeletal muscle model. The proposed mathematical model is suitable for a 3D muscle representation. It respects the microstructure of the muscle which is represented by three basic components: active fibers, passive fibers and a matrix. For purposes of presented work the existing material models suitable for the matrix and passive fibers are used and a new active fiber model is proposed. The active fiber model is based on the sliding cross-bridge theory of contraction. This theory is often used in modeling of skeletal and cardiac muscle contractions. In this work, a certain simplification of the cross-bridge distribution function is proposed, so that the 3D computer implementation becomes feasible. The new active fiber model is implemented into our research finite element code. A simple 3D muscle bundle-like model is created and the implemented composite model (involving the matrix, passive and active fibers) is used to perform the isometric, concentric and excentric muscle contraction simulations.
© 2009 University of West Bohemia. All rights reserved.

Keywords: skeletal muscle, cross-bridge distribution, calcium activation, fiber architecture, composite model

1. Introduction

Computer simulations of various human body functions have already shown a wide applicability in many branches of medicine, sports or vehicle safety research. The human body modeling respects two concepts in general. The first one is based on a tissue microstructure and enables a detailed modeling of body parts, while the second one models a human body as a whole usually in the interaction with surroundings. These two concepts complement each other.

This paper deals with modeling of skeletal muscle tissue and focuses on the detailed description of active properties. It provides a compact summary of the investigated problem including the relations presented in [11] completed by several essential conditions. The model is implemented into the MAFEST (Matlab Finite Element Simulator) software that is being developed at our laboratory, see [2]. MAFEST is a modular software suitable for various modeling tasks in biomechanics. Recently it has been used for implementation of smooth and cardiac muscle tissue modeling, together with the related sensitivity algorithm for material parameters identification, cf. [3, 17, 18]. The identification algorithm was used for smooth muscle tissue [13] and kidney [4] parameter determination.

The active fiber model is based on the cross-bridge kinetics (sometimes also called theory of sliding filaments) introduced firstly by Huxley [9] which was further extended or used by

---

*Corresponding author. Tel.: +420 377 634 710, e-mail: hcechov@ntc.zcu.cz.

many other authors, cf. [6, 15, 19]. The paper introduces an advanced active fiber model which in connection with a proper model of passive fibers and matrix gives a suitable 3D composite skeletal muscle representation.

2. Anatomical background

Following paragraphs give a brief summary of a skeletal muscle anatomy and a physiology of muscle contraction ease to a reader the orientation in a number of terms.

2.1. Skeletal muscle structure

Skeletal muscles can be described from the macroscopic and the microscopic points of view. We start with the macroscopic one. A long multinucleate fiber is a basic constructive element of each skeletal muscle that is important for this approach. Muscle fibers are then joined to a primary bundle and the parallel oriented bundles form a muscle.

At the microscopic level the fiber can be further divided into *myofibrils*, each containing a number of *filaments*. The cytoplasm, often called *sarcoplasm*, of the muscle filamentum involves many actual contractile elements called *sarcomeres*. The basis of each sarcomere is created by the thin filaments containing the protein *actin* and the thick filaments containing the protein *myosin*. They fit together and create so called *cross-bridges* which enable a mutual movement causing the contraction of the sarcomere, see fig. 1, left. The thin filaments of adjacent sarcomeres are anchored in so called Z-discs. The regular structure of Z-discs is responsible for a striated appearance of the skeletal muscle. The sarcomere structure is outlined in fig. 1, right.

2.2. Contraction cycle

The contraction occurss when the cross-bridges between actin and myosin bind and generate a force causing the thin filaments to slide along the thick filaments. According to the sliding filament theory the sarcomere force depends on the amount of overlaps of the actin and myosin filaments.
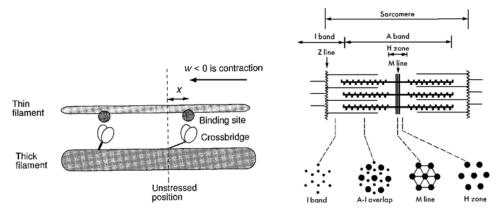

Fig. 1. Bonding of a cross-bridge (left), sarcomere structure(right); taken from [10]

The optimum sarcomere (fiber, muscle) length is the length when the overlap of the actin and myosin filaments enables the interaction of all cross-bridges and consequently the generated force touches its peak. With increasing muscle length the number of cross-bridges decreases. For lengths smaller than the optimum length, actin filaments overlap and the number of cooperating cross-bridges again decreases.

The passive force contributes also to the total force for lengths over a passive slack length, i.e. the smallest length when any force is exerted under passive conditions. The contraction is a very complicated cycle, which stands upon the creation and conversion of ATP and on the transfer of calcium ions, cf. [1, 10].

3. Composite model of skeletal muscle

The proposed model consists of a matrix, active fibers and passive fibers. A new active fiber model, whose incomplete version was introduced in [11], is implemented. The hyperelastic material model for the matrix and viscoelastic passive fibers with linear elastic response are chosen from the MAFEST library. The proposed active fiber model arises from a sliding cross-bridge theory of contraction, cf. [10], which is often used in skeletal and cardiac muscle modeling.

3.1. General setting

Below we use the following notation: vectors: $\square$ with components $\{\square_i\}$, $i = 1, 2, 3$; second order tensors: $\underline{\underline{\square}}$ with components $\{\square_{ij}\}$, $i, j = 1, 2, 3$.

The composite model assumes that at any point in the material the properties of the solid reflect the microstructure. The microstructure of muscle is characterized by three basic components: *active fibers* representing bundles of muscle cells, *passive fibers* corresponding to collagen and elastin fibers and finally a *matrix* substituting the amorphous extracellular substance. These components are supposed to occupy an infinitesimal volume according to the volume fractions denoted by ϕ^a, ϕ^p and ϕ^m respectively, so that

$$\phi^a + \phi^p + \phi^m = 1. \tag{1}$$

All the components contribute then to the total stress in proportion to their volume fractions, cf. [16]. Large deformations exhibited by the muscle tissue are described using the total Lagrangian formulation (TLF). The total second Piola–Kirchhoff stress tensor $\underline{\underline{S}}$ is represented by the summation of the contributions of each component which are proportional to the associated volume fractions:

$$\underline{\underline{S}} = \phi^m \underline{\underline{S}}^m + \phi^p \underline{\underline{\tau}}^p + \phi^a \underline{\underline{\tau}}^a, \tag{2}$$

where $\underline{\underline{S}}^m$ is the matrix stress, $\underline{\underline{\tau}}^p$ and $\underline{\underline{\tau}}^a$ are the stress tensors of fibrous components. Similar composite model types are described for example in [8]. At any point of the continuum the model enables both active and passive fibers to be distributed in several preferential directions k in which the tension can be transmitted, k belongs to the index set I^a in case of the active fibers and to the index set I^p for the passive fibers. The kth direction is defined by the unit vector $v^k = (v_1^k, v_2^k, v_3^k)$ related to the undeformed configuration. A quantity of active fibers in the kth direction is proportional to the volume fraction ϕ_a^k, $\sum_{k \in I^a} \phi_a^k = 1$ and analogously for the passive fibers. Using the directional tensor $\omega_{ij}^k = v_i^k v_j^k$ the stress tension of fibrous components can be expressed as

$$\underline{\underline{\tau}}^p = \sum_{k \in I^p} \phi_p^k \tau_p^k \underline{\underline{\omega}}^k, \qquad \underline{\underline{\tau}}^a = \sum_{k \in I^a} \phi_a^k \tau_a^k \underline{\underline{\omega}}^k \tag{3}$$

(indexes ij omitted). Hence the fibrous components introduce *strong anisotropy* to the model.

We are interested mainly in quasi-static solutions and we omit in the following the inertia terms. Assuming the solution up to the step n to be known, we seek the solution at the step $n + 1$ satisfying the equilibrium equation

$$\int_{\Omega^{(0)}} \underline{\underline{S}}^{(n+1)} : \delta \underline{\underline{E}}(\underline{v}) \, \mathrm{d}\Omega - L^{(n+1)}(\underline{v}) = 0, \quad \forall \underline{v} \in V^3, \tag{4}$$

where $\underline{\underline{E}}$ is the Green deformation tensor, L represents linear loads and V is a suitable function space. The Green deformation tensor can be expressed using the deformation gradient $\underline{F}$ as $\underline{\underline{E}} = 1/2(\underline{F}^T\underline{F} - \underline{I}) = 1/2(\underline{C} - \underline{I})$. Here $\underline{F}$ relates the spatial coordinates $\underline{x}$ to the material ones $\underline{X}$ by $\underline{F} = \frac{\partial \underline{x}}{\partial \underline{X}}$, $\underline{C}$ is the right Cauchy-Green deformation tensor, $\underline{C} = \underline{F}^T\underline{F}$ and $\underline{I}$ is the identity.

3.2. Matrix

A rather simple hyperelastic material model is chosen for the matrix, substituting the extracellular substance, since only small contribution of the matrix to the mechanical behavior of the complex tissue is considered, which was proved sufficient in similar models, cf. [5] and [14]. To respect the nearly incompressibility of soft tissues it is convenient to split the $\underline{S}^m$ into the effective (shear) part $\underline{S}^{eff}$ and the volumetric (pressure) part $-pJ\underline{C}^{-1}$ with $J = \det(\underline{F})$. The incompressibility is treated using common definition $p = -K(J - 1)$, where K is the bulk modulus.

In our model the matrix is represented by the hyperelastic material, the second Piola Kirchhof stress tensor can be obtained as

$$\underline{\underline{S}}^m = \frac{\partial W}{\partial \underline{\underline{E}}}. \tag{5}$$

W denotes the strain energy which can have various forms according to a type of material. The simplest hyperelastic material, the neo-Hookean, was chosen:

$$\underline{\underline{S}}^m = \underline{\underline{S}}^{eff} - pJ\underline{C}^{-1} = \mu J^{-\frac{2}{3}}(\underline{I} - \frac{1}{3}\text{tr}(\underline{C})\underline{C}^{-1}) + K(J - 1)J\underline{C}^{-1}, \tag{6}$$

where the shear modulus μ and the bulk modulus K are the material parameters.

3.3. Passive fibers

The passive fibers characterize the collagen and elastin network in the muscle tissue which shows nonlinear viscoelastic behavior. The fibers transmit only tension. The viscoelastic passive fibers with linear elastic response are chosen from the MAFEST material library [2]. This type of passive fibers is represented by the uniaxial three parametric Kelvin-Zener model. The viscoelastic stress τ^p (in the following the superscript p omitted for brevity) is a function of the elastic response σ and the internal stress-like variable q and it is expressed as

$$\tau = \sigma - q, \tag{7}$$

$$\dot{q} + \frac{1}{T_\epsilon}q = \frac{\gamma}{T_\epsilon}\sigma \tag{8}$$

where T_ϵ is the relaxation time and γ is the relaxation parameter. At the thermodynamic equilibrium ($\dot{q} = 0$) from 7 and 8 one can obtain an explicit formula for $\sigma(t)$

$$\sigma(t) = \frac{1}{1 - \gamma}\left(\tau(t) - \gamma\int_{t_0}^t e^{-\beta(t-s)}\frac{\mathrm{d}\tau(s)}{\mathrm{d}s}\,\mathrm{d}s\right) \tag{9}$$

where $\beta = (1 - \gamma)T_\epsilon$. The elastic response is given always by the instantaneous strain $\varepsilon_p(t)$ obtained from displacement field. A very simple linear elastic response can be defined as

$$\sigma(t) = D\varepsilon_p(t)(t) \tag{10}$$

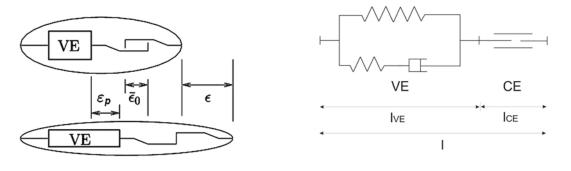where D denotes a positive constant.

Fig. 2. Passive fiber

Fig. 3. Schema of the active fiber model

The collagen fibers are tangled in helical bundles in the undeformed tissue. Consequently they can transmit tension only after their straightening, while in compression they cannot transmit any load. This behavior is taken into account by the relative slack length parameter $\bar{\epsilon}_0$ depicted in Fig. 2 and expressed by the following relations:

$$\varepsilon_p(t) \geq \epsilon(t) - \bar{\epsilon}_0$$

$$\tau(t) \geq 0 \tag{11}$$

$$\tau(t) \cdot (\varepsilon_p(t) - \epsilon(t) + \bar{\epsilon}_0) = 0$$

where $\bar{\epsilon}_0 \geq 0$ allows taking into account the waviness of collagen fibers in released state and $\bar{\epsilon}_0 < 0$ corresponds to residual stresses.

3.4. Active fiber model

The active fiber model employs ideas from a sliding cross-bridge theory of contraction. This theory also known as the kinetic theory, was firstly proposed by A. F. Huxley already in 1957 and later it was extended by many other authors. The principles are based on modeling of bonding and debonding cross-bridges between actin and myosin filaments. Major activities were focused on the development of constitutive equations for description of the calcium activation and cross-bridge bonding/debonding process. Fundamental seems to be a work [19] where an approximation of a cross-bridge distribution function describing the kinetic theory was introduced.

The muscle tissue besides contains active filaments, as well the material embodying the viscoelastic behavior. Hence our model is constituted of the contractile element (CE) in series with viscoelastic element (VE), see fig. 3. The VE respects the Kelvin-Zener rheological model, the CE model arises from the Huxley type two state model.

3.5. Contractile part of active fiber

The constitutive equation of the contractile myofibers is based on the micro-mechanical Huxley model. The simplest model of Huxley type assumes that the cross-bridges have only two possible states: bonded and debonded. The bonded cross-bridge generates a force that causes shortening of the sarcomere. The distribution of attached cross-bridges with respect to their length ξ is given by the function $n(\xi, t)$:

$$\frac{\partial n(\xi, t)}{\partial t} - w(t)\frac{\partial n(\xi, t)}{\partial \xi} = r(t)f(\xi)\left(\alpha - n(\xi, t)\right) - g(\xi)n(\xi, t), \tag{12}$$

where w represents the macroscopic shortening velocity [20], α denotes the overlap function:

$$\alpha\left(\frac{\lambda_{CE}}{\lambda_{opt}}\right) = \begin{cases} 1 - 6.25\left(\frac{\lambda_{CE}}{\lambda_{opt}} - 1\right)^2 & \text{for} \quad \frac{\lambda_{CE}}{\lambda_{opt}} \leq 1, \\ 1 - 1.25\left(\frac{\lambda_{CE}}{\lambda_{opt}} - 1\right) & \text{for} \quad \frac{\lambda_{CE}}{\lambda_{opt}} > 1, \end{cases} \tag{13}$$

where λ_{CE} represents the ratio of instantaneous contractile element length l_{CE} and rest contractile element length L_{CE}, λ_{opt} is the optimal stretch. The function $f(\xi)$ is the attachment rate function and $g(\xi)$ is the detachment rate function of actin to myosin. Both of them are defined according to [19].

The activation factor r in (12) represents the fraction of sites on the actin filament that is activated. This activation occurs if the corresponding troponin site of the attachment sites is unlocked by two calcium ions. The activation factor r is determined from the chemical equilibrium between calcium and troponin and it is expressed as:

$$r = \frac{C^2}{C^2 + \mu C + \mu^2}, \tag{14}$$

with C the calcium concentration in the myofibrilar space normalized with respect to the maximum myofibrilar calcium concentration and μ the troponin-calcium reaction ratio constant. The rate of change of the normalized calcium concentration in the myofibrilar space is defined according to [7]:

$$\frac{\partial C}{\partial t} = \vartheta(c\nu - C), \tag{15}$$

where ϑ stands for the fiber-type dependent rate parameter, c is the calcium release parameter and ν ($\nu = f/f_{max}$) is the stimulation frequency f normalized by the tetanic stimulation frequency f_{max}.

In the Huxley theory a bound cross-bridge is supposed to behave like a spring. The contractile stress developed by all cross-bridges in a slice of half sarcomeres is:

$$\sigma_{CE} = K_A \int_{-\infty}^{\infty} \xi n(\xi, t)\,\mathrm{d}\xi = K_A Q_1(t) \tag{16}$$

with K_A a material constant. The term Q_1 is the first moment of the distribution function $n(\xi, t)$.

3.6. Simplified distribution-moment approximation

The equation (16) shows that the contractile stress does not depend on the exact shape of $n(\xi, t)$ but it is proportional to the first order distribution moment of $n(\xi, t)$. The kth distribution moment (DM) of $n(\xi, t)$ is generally defined as:

$$Q_k(t) = \int_{-\infty}^{\infty} \xi^k n(\xi, t)\,\mathrm{d}\xi \qquad k = 0, 1, 2, \ldots \tag{17}$$

This idea was first used by Zahalak and published in [19]. The DM method transforms the partial differential equation (12) to a set of first-order ordinary differential equations:

$$\frac{\partial Q_k}{\partial t} = \alpha r \beta_k - r\phi_{k1} - \phi_{k2} - kwQ_{k-1} \qquad k = 0, 1, 2, \ldots \tag{18}$$

with the integrals

$$\beta_k = \int_{-\infty}^{\infty} \xi^k f(\xi) \, d\xi, \quad \phi_{k1} = \int_{-\infty}^{\infty} \xi^k f(\xi) n(\xi, t) \, d\xi, \quad \phi_{k2} = \int_{-\infty}^{\infty} \xi^k g(\xi) n(\xi, t) \, d\xi. \quad (19)$$

If the approximation of $n(\xi, t)$ is chosen suitably then the system (18) becomes explicit for the moments Q_k.

In [19] the Gaussian approximation is chosen as a proper approximation of participating cross-bridge distribution. Thus $n(\xi, t)$ is characterized by its first three moments Q_0, Q_1, Q_2:

$$n(\xi, t) = \frac{Q_0}{\sqrt{2\pi} q(t)} e^{-\frac{(\xi - p)^2}{2q^2}}, \quad (20)$$

$$p = \frac{Q_1}{Q_0} \quad \text{and} \quad q = \sqrt{\frac{Q_2}{Q_0} - \left(\frac{Q_1}{Q_0}\right)^2}, \quad (21)$$

As a result a system of three first-order ordinary differential equations is obtained instead of partial differential equation.

Substituting the Gaussian approximantion of $n(\xi, t)$ into integrals ϕ_{k1} and ϕ_{k2} we obtain expressions involving the error function, see [19]. Their computer implementation is rather complicated. Hence it is convenient to further approximate the Gaussian approximation of $n(\xi, t)$ with a polynomial function. In [11] we proposed to approximate $n(\xi, t)$ by two cubic spline functions:

$$n(\xi, t) = c_0 + c_1 \xi + c_2 \xi^2 + c_3 \xi^3, \quad (22)$$

where the coeficients c_i $(i = 0, \ldots, 3)$ depend on the moments Q_0, Q_1, Q_2.

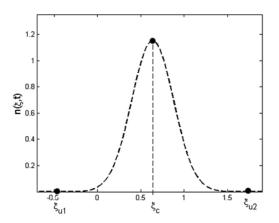

Fig. 4. Gaussian distribution of $n(\xi, t)$. Signed nodes ξ_c and ξ_u are used for determining an appropriate spline function

Each segment of the spline respects the maximum value (ξ_c) of the Gaussian distribution of $n(\xi, t)$ and the point (ξ_u) where $n(\xi, t)$ is close to zero. These values are displayed in fig. 4. The maximal value of $n(\xi, t)$ is attained for ($\xi_c = p$), where p is defined in (21). The coefficients c_i follow from conditions for values of function and their first derivatives in the end points of the interval (ξ_u, ξ_c):

$$\begin{bmatrix} 1 & \xi_c & \xi_c^2 & \xi_c^3 \\ 1 & \xi_u & \xi_u^2 & \xi_u^3 \\ 0 & 1 & 2\xi_c & 3\xi_c^2 \\ 0 & 1 & 2\xi_u & 3\xi_u^2 \end{bmatrix} \begin{bmatrix} c_0 \\ c_1 \\ c_2 \\ c_3 \end{bmatrix} = \begin{bmatrix} n(\xi_c) \\ 0 \\ 0 \\ 0 \end{bmatrix}. \quad (23)$$
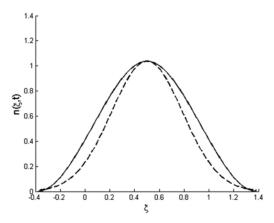
Fig. 5. Comparison of Gaussian approximation (dashed lines) to spline approximation (solid lines) of $n(\xi, t)$
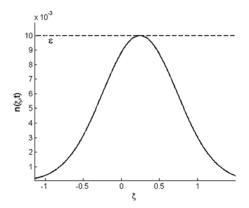

Fig. 6. Gauss. distrib. of $n(\xi, t)$ for small Q_i (solid line) with the limit ε (dashed line)

Solving (23) gives:

$$c_0 = \frac{Q_0}{\sqrt{2\pi}} \frac{\xi_u^2(3\xi_c - \xi_u)}{(\xi_c - \xi_u)^3 \sqrt{Q_2/Q_0 - (Q_1/Q0)^2}}, \tag{24}$$

$$c_1 = -\frac{Q_0 3\sqrt{2}}{\sqrt{\pi}} \frac{\xi_c \xi_u}{(\xi_c - \xi_u)^3 \sqrt{Q_2/Q_0 - (Q_1/Q0)^2}}, \tag{25}$$

$$c_2 = \frac{Q_0 3}{\sqrt{2\pi}} \frac{\xi_c + \xi_u}{(\xi_c - \xi_u)^3 \sqrt{Q_2/Q_0 - (Q_1/Q0)^2}}, \tag{26}$$

$$c_3 = \frac{Q_0\sqrt{2}}{\sqrt{2\pi}} \frac{1}{(\xi_c - \xi_u)^3 \sqrt{Q_2/Q_0 - (Q_1/Q0)^2}}, \tag{27}$$

where the limit value ξ_u fulfills the assumption:

$$\xi_u : \qquad n(\xi_u, t) < \varepsilon \ll 1. \tag{28}$$

Solving (28) we obtain the expression for ξ_u which is a function of distribution moments:

$$\xi_{u1} > p - q\sqrt{2}\sqrt{-ln\frac{\varepsilon}{a_0}}, \qquad \xi_{u2} < p + q\sqrt{2}\sqrt{-ln\frac{\varepsilon}{a_0}}, \tag{29}$$

with $a_0 = \frac{Q_0}{q\sqrt{2\pi}}$ and $\xi_u = \xi_{u1}$ corresponding to the left spline branch and $\xi_u = \xi_{u2}$ to the right spline branch. Fig. 5 demonstrates the comparison of the Gaussian approximation and the spline approximation of $n(\xi, t)$. Moreover (21) and (28) give rise to four conditions of solvability:

$$\frac{Q_0}{\sqrt{2\pi}q} > 0, \qquad q > 0, \qquad Q_0 Q_2 \leq Q_1^2 \frac{Q_0}{\sqrt{2\pi}q} < \epsilon. \tag{30}$$

Note that the conditions (30) do not limit the possible solutions. They correspond to physical principles: fiber stiffness and generated force are greater than zero. The first three conditions hold also for the Gaussian approximation, which is fitted to the experiment, the last one arises from the spline approximation. If the last condition does not hold, it means that all Q_i are small and the situation displayed in fig. 6 occurs. In such a case it is possible to decrease ε, so that this condition does not resctrict the solution.
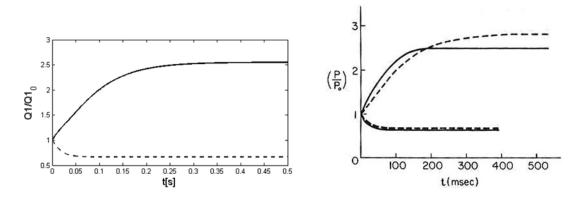
Fig. 7. Comparison of stretch and release response of the original Huxley model (solid lines) and the DM approximation (dashed lines) with the Gaussian approximation of $n(\xi, t)$ (right, taken from [19]) and the DM approximation with the spline approximation of $n(\xi, t)$ (left), constant velocity $w = \pm 10\,\mathrm{s}^{-1}$.

The behavior of the selected spline approximation was tested for correctness on a simple example and it was compared to a test published in [19]. The results are concluded by the graphs in fig. 7, with the first distribution moment displayed on the vertical axis normalized by its initial condition. For this comparison the initial conditions and parameters were set the same as in [19].

3.7. Equilibrium of active and passive elements

The passive properties of the muscle tissue, which are associated to the connective tissue components, are simulated by a viscoelastic component in series with the contractile element [17], recall fig. 3. The total stretch of the active fiber is the summation of its two components:

$$\lambda = \frac{l}{L} = c_{CE}\lambda_{CE} + c_{VE}\lambda_{VE} = c_{CE}\frac{l_{CE}}{L_{CE}} + c_{VE}\frac{l_{VE}}{L_{VE}}, \tag{31}$$

where l_{CE}, l_{VE} denote the instantaneous and L_{CE}, L_{VE} the rest lengths of particular components with the coefficients c_{CE}, c_{VE}. According to [17] it is assumed that w is proportional to λ_{CE}. It is necessary to note that w is defined as contraction while λ_{CE} represents elongation, therefore

$$w = -c_w\dot{\lambda}_{CE}, \tag{32}$$

with c_w a proportional coefficient.

The stress response of the VE obeys:

$$\tau(t, \lambda_{VE}) = (1-\gamma)\sigma(\lambda_{VE}(t)) + \gamma\int_0^t \mathrm{e}^{-(t-\theta)/T}\dot{\sigma}(\lambda_{VE}(\theta))\,\mathrm{d}\theta, \tag{33}$$

$$\sigma(\lambda_{VE}) = E(\lambda_{VE}-1) = E\left(\frac{\lambda - c_{CE}\lambda_{CE}}{c_{VE}} - 1\right), \tag{34}$$

where σ_{CE} is the linear elastic response with E the Young modulus, γ is the relaxation parameter and T the relaxation time.

As CE and VE are connected in series, they transmit the same tension and the whole element is in the equilibrium:

$$\tau(\lambda, \lambda_{CE}, t) = \sigma_{CE}(\lambda_{CE}, t). \tag{35}$$

If the total deformation λ is given then λ_{CE} can be computed from the equilibrium equation (35) and λ_{VE} satisfies (31).

4. Implementation of the complete model into MAFEST

The material model of the active skeletal muscle fiber described in the previous sections was implemented into MAFEST. This software is based on the combination of two programming languages: Matlab and C, cf. [2]. The program core containing material definitions and FE assembling is written in C. The user interface and the program logic are implemented in Matlab.

Recall that our material is a composite mixture (CM) consisting of three plys: a hyperelastic matrix, passive fibers and active fibers where, according to the theory of mixtures, the total stress of the material is the sum of stresses of particular plys weighted by their volume fractions as stated in (2). All plys share a common displacement field and no mutual movement is considered, see [2], where the constitutive relations for matrix and passive fibers are described in detail. The active fiber stress is defined by (16).

We assume our problem is discretized in space by finite elements (FE) [2]. In the TLF, all quantities and integrals are related to the initial configuration which is undeformed and the space derivatives are with respect to the material coordinates $\underline{X}$. The displacements $\underline{u}$ represent the unknown field, $\underline{x} = \underline{X} + \underline{u}$, $\underline{x} = \boldsymbol{\chi}^T \cdot \boldsymbol{x}$, $\underline{u} = \boldsymbol{\chi}^T \cdot \boldsymbol{u}$ and $\boldsymbol{\chi}$ are the FE base functions. In particular the tri-linear base functions are used in the numerical examples below with the hexahedral finite elements.

The integral in the weak form of the equilibrium equation (4) is evaluated numerically over each finite element using a numerical (Gauss) quadrature. Thus all the material parameters must be given in all the quadrature points in the whole domain. In MAFEST, any parameter, in particular the fibre directions, can be defined independently in each quadrature point, allowing for the inhomogeneity and anisotropy of the tissue. The internal equilibrium of the active fiber is solved in each quadrature point separately too.

The equilibrium equation of the CM is expressed below by the function $\boldsymbol{f}$ (discrete counterpart of (4)) and h corresponds to the internal equilibrium of the active fiber (discrete counterpart of (35)):

$$\boldsymbol{f}(\dot{\boldsymbol{u}}, \boldsymbol{u}, \boldsymbol{\lambda}_{CE}) = 0, \qquad \boldsymbol{u} = \{u_j\}_1^{n_u}, \tag{36}$$

$$h(\boldsymbol{u}, \boldsymbol{\lambda}_{CE}) = 0, \qquad \boldsymbol{\lambda}_{CE} = \{\lambda_{CEj}\}_1^{n_Q}, \tag{37}$$

where n_u is the number of displacement degrees of freedom per element, n_Q is the number of quadrature points per element and λ_{CE} is the internal variable in quadrature points.

The discretized second Piola-Kirchhoff stress tensor $\underline{S}$ in vector form is denoted by $\boldsymbol{s}$. Then in the FE discretization the term $\delta_u \underline{E}(\underline{u}; \underline{v})$ turns into

$$\delta_u \underline{E}(\underline{u}; \underline{v}) \approx \boldsymbol{B}(\boldsymbol{u}) \cdot \boldsymbol{v}, \tag{38}$$

and the equations (36), (37) can be written in the form

$$\boldsymbol{f}(\boldsymbol{u}, \boldsymbol{\lambda}_{CE}) := \sum_{q=1}^{n_Q} [\boldsymbol{B}(\boldsymbol{u})^T \cdot \boldsymbol{s}(\boldsymbol{u}, \lambda_{CE}) J_0] = 0, \tag{39}$$

$$h_{|q} := \sigma_{CE}(\lambda_{CE}) - \tau(\lambda, \lambda_{CE}) = 0, \qquad q = 1 \dots n_Q, \tag{40}$$

where the total stress $\boldsymbol{s}$ for $q = 1 \dots n_Q$ (index omitted) is

$$\boldsymbol{s}(\boldsymbol{u}, \lambda_{CE}) := \phi^m \boldsymbol{s}^m(\boldsymbol{u}) + \phi^a \tau^a(\boldsymbol{u}, \lambda_{CE}) \boldsymbol{\omega} + \phi^p \tau^p(\boldsymbol{u}) \boldsymbol{\omega}. \tag{41}$$
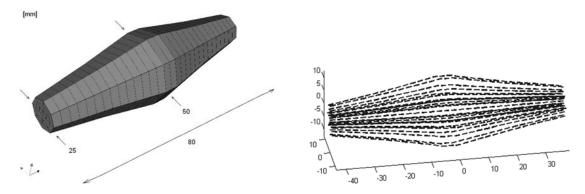
Fig. 8. Muscle bundle in the undeformed state (left), fiber orientation (right)

Assuming the time discretization, for the step $n + 1$ we obtain:

$$\boldsymbol{f}(\boldsymbol{u}^{(n+1)}, \lambda_{CE}^{(n+1)}) := \sum_{q=1}^{n_Q} [\boldsymbol{B}(\boldsymbol{u}^{(n+1)})^T \cdot \boldsymbol{s}(\boldsymbol{u}^{(n+1)}, \lambda_{CE}^{(n+1)}) J_0]_{|\underline{\xi}^q} = 0, \qquad (42)$$

$$h_{|q} := \sigma_{CE}(\lambda_{CE}^{(n+1)}) - \tau(\lambda^{(n+1)}, \lambda_{CE}^{(n+1)}) = 0, \qquad q = 1 \ldots n_Q, \qquad (43)$$

where the discretized equation for defining $h_{|q}$ is itemized in detail in [12]. The nonlinear problem (36)–(37) is solved by the Newton method. The above equations, related to a single finite element, are assembled for the whole discrete domain in the usual finite element sense.

5. Examples

The validation of the active fiber material model according to tests presented in literature can be found in [11] or [12]. In our case the whole implemented skeletal muscle model is tested on a simple muscle-like geometry. The shape reminding a muscle bundle is depicted undeformed in fig. 8, left. Both the active and passive fibers are defined in the longitudinal direction as is shown in fig. 8, right. The small model dimensions are chosen due to fact that all parameters found in literature [6, 7, 19] are measured on small specimens (frog or rats). The used parameters of active fibers are summarized in Tab. 1, where f_1, g_1, g_2 and g_3 belong to the attachment and detachment rates $f(\xi)$, $g(\xi)$.

Table 1. Active fiber parameters

Contractile element							Viscoelatic element		
f_1 [s^{-1}]	g_1 [s^{-1}]	g_2 [s^{-1}]	g_3 [s^{-1}]	θ [s^{-1}]	μ [–]	K_A [kPa]	γ [–]	E [kPa]	T [s^{-1}]
35	7	200	30	11.25	0.2	400	0.75	10^4	0.1

The isometric contraction of the muscle model lasting 0.5 s is displayed in fig. 9 (a). The reaction to the external loading which is lower (4 kPa) than the maximal force generated by the muscle, is denoted as the concentric contraction and can be seen in fig. 9 (b). While the excentric contraction occurs when the external loading is greater than the maximal force generated by the muscle (20 kPa) and is presented in fig. 9 (c).

In all previous simulations the muscle model swells in its middle part. It is caused by the uniform distribution of the active fiber parameter K_A. This parameter is related to the fiber

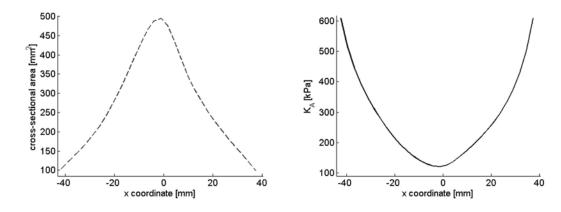Fig. 9. Isometric (a), concentric(b) and excentric (c) contraction; constant K_A

Fig. 10. Cross-section area along the bundle (left), distribution of K_A for $\text{const} = 60\,000$
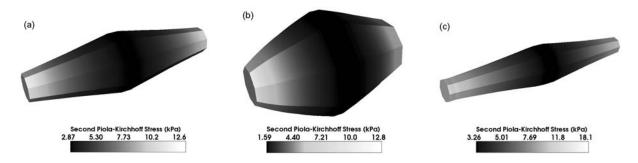

Fig. 11. Isometric (a), concentric and excentric (c) contraction; $K_A = K_A(x)$

cross-section, which causes that the greater cross-sectional area contains more active fibers. In consequence the active force generated in the middle of the bundle is greater due to this greater cross-sectional area. However according to anatomy sources a muscle bundle contains a constant number of fibers in an arbitrary cross-section, i.e. any muscle bundle generates a constant force through its cross sections. Thus we define a K_A as a function $K_A = K_A(x)$, such that the generated force remains constant and x changes along the muscle:

$$K_A(x) = \frac{\text{const}}{S(x)}, \tag{44}$$

where $S(x)$ is the cross-sectional area dependent on the longitudinal coordinate x, see fig. 10.

The previous examples are now recomputed with K_A dependent on the cross-sectional area. As depicted in fig. 11 (a), the isometric contraction is now without the "belly effect", the strains are very small. For the comparison see also fig. 11 (b) and (c) where the concentric and excentric contractions are displayed.

6. Conclusion

The paper deals with the 3D skeletal muscle modeling. The muscle tissue is formed by a matrix, passive fibers and active fibers. The implementation of the model uses the constitutive relations provided by MAFEST for the passive fiber and the matrix, and for the active fibers the new material model.

The active fiber behavior is based on the Huxley type model respecting the tissue microstructure and involving the calcium activation. The fiber microstructure is represented by a function describing the actual distribution of bonded cross-bridges. The new approximation of the cross-bridge distribution function leading to the easier computer implementation was proposed.

The simple muscle bundle-like geometry was created and the isometric concentric and excentric contractions of our 3D muscle model were shown. The presented model is able to simulate various situations during muscular contraction. It is also possible to apply the model to an arbitrary geometry and respect the fiber architecture. It is suitable for modeling of isolated muscles. However the implementation into a whole body model is not effective because of its high computational complexity.

Acknowledgements

References

[1] Bannister, L. H., Berry, M. M., Collins, P., Dussek, J. E., Dyson, M., Gray's Anatomy, Churchil Livingstone, Great Britain, 1995.

[2] Cimrman, R., Mathematical modeling of biological tissues, Ph.D. thesis, University of West Bohemia, Pilsen, 2002.

[3] Cimrman, R., Rohan, E., Modelling heart tissue using a composite muscle model with blood perfusion, Proceedings of Computational Fluid and Solids Mechanics 2003, Elsevier Science Ltd., 2003.

[4] Cimrman, R., Rohan, E., Nováček, V., Mechanical modelling and parameter identification of soft tissue: Kidney case study, Proceedings of Computational Mechanics 2005, Hrad Nečtiny, University of West Bohemia, Pilsen, 2005, pp. 111–118.

[5] Cimrman, R., Rohan, E., On identification of the arterial model parameters from experiments applicable "in vivo", Mathematics and Computers in Simulation (2009), in press.

[6] Gielen, A. W. J., A continuum approach to the mechanics of contracting skeletal muscle, Ph.D. thesis, Eindhoven University of Technology, 1998.

[7] Hatze, H., Myocybernetic control models of skeletal muscle: Characteristics and applications, University of South Africa, Muckleneuk, Pretoria 1981.

[8] Holtzapfel, G. A., Nonlinear Solid Mechanics, John Wiley & Sons Ltd., England, 2000.

[9] Huxley, A. F., The mechanism of muscular contraction, Science 164 (1969) 1 356–1 366.

[10] Keener, J., Sneyd, J., Mathematical Physiology, Springer-Verlag, NewYork, 1998.

[11] Kocková, H., Cimrman, R., On skeletal muscle model with new approximation of cross-bridge distribution, Proceedings of Computational mechanics, Hrad Nečtiny, University of West Bohemia, 2006, pp. 255–260.

[12] Kocková, H., Biomechanical models of living tissues and their industrial applications, Ph.D. thesis, University of West Bohemia, Pilsen, 2007.

[13] Kochová, P., Cimrman., R., Rohan, E., Parameter identification and mechanical modelling of smooth muscle and connective tissue, Proceedings of Applied mechanics 2007, Technical University of Ostrava, Ostrava, 2007, pp. 133–135.

[14] Kochová, P., Cimrman, R., Rohan, E., Orientation of smooth muscle cells with application in mechanical model of gastropod tissue, Applied and Computational Mechanics 3, (2009), in press.

[15] Oomens, C. W. J., Maenhout, M., van Oijen, C. H., Drost, M. R., Baaijens, F. P., Finite element modelling of contracting skeletal muscle, The Royal Society 358 (2003) 1 453–1 460.

[16] Rohan, E., Cimrman, R., Numerical simulation of activated smooth muscle behaviour using finite elements, Proceedings of UWB, University of West Bohemia, Pilsen, 1999, pp. 143–155.

[17] Rohan, E., On coupling the sliding cross-bridge model of muscle with series viscoelastic element, Proceedings of Computational Mechanics, Hrad Nečtiny, University of West Bohemia, Pilsen, 2002, pp. 395–402.

[18] Sainte-Marie, J., Chapelle, D., Cimrman, R., Sorine, M., Modeling and estimation of the cardiac electromechanical activity, Computers and Structures 84 (2006) 1 743–1 759.

[19] Zahalak, G. I., A distributed moment approximation for kinetic theories of muscular contraction, Mathematical Biosciences 55 (1981) 89–114.

[20] Zahalak, G. I., Ma, S. P., Muscle activation contraction: constitutive relations based directly on cross-bridge kinetics, Journal of Biomechanical Engineering 112 (1990) 52–62.

[21] World of the Body: skeletal muscle, http://www.answers.com/topic/skeletal-muscle.